IL NUOVO CIMENTO **43 C** (2020) 18
DOI 10.1393/ncc/i2020-20018-3

COLLOQUIA: FATA 2019

Use of Cherenkov light in TOF-PET

R. PESTOTNIK
Jožef Stefan Institute - Ljubljana, Slovenia

received 2 March 2020

Summary. — The time-of-flight resolution of PET scanners is limited by the timing spread due to delayed scintillation emission. By using prompt Cherenkov photons instead, the coincidence timing resolution can be improved. The improvement is limited by the photon travel time spread in the crystals. By segmenting the crystals, the remaining contribution is due to the intrinsic time resolution of the photosensors. In this contribution, we evaluate the feasibility of using lead fluoride in Cherenkov-light–based PET scanner with silicon photomultipliers. Due to a significantly lower price of lead fluoride compared to an L(Y)SO scintillator, such a scanner is a competitive option already with the use of current silicon photomultipliers which have a single photon time spread of around 100 ps.

1. – Introduction

A Cherenkov light is emitted when a charged particle is moving in a medium with refractive index n with a velocity of $v = \beta c$ exceeding the speed of light $\frac{c}{n}$ in that medium. The produced polarized light is emitted at a characteristic (Cherenkov) angle θ_{Ch} which depends on the particle velocity and refractive index as

$$\cos\theta_{Ch} = \frac{c}{nv} = \frac{1}{\beta n}. \tag{1}$$

The number of emitted photons per unit length $\frac{\mathrm{d}N}{\mathrm{d}l}$ also depends on the particle velocity indirectly through the dependance on the θ_{Ch} as

$$\frac{\mathrm{d}N}{\mathrm{d}l} = \frac{\alpha}{\hbar c}\sin^2\theta_{Ch}. \tag{2}$$

The phenomenon is extensively used in high energy physics for particle identification of elementary particles. In Ring Imaging Cherenkov detectors, the emitted single photons are detected by very low-noise and highly efficient position photosensitive detectors enabling measurement of the Cherenkov angle, from which, together with the measured

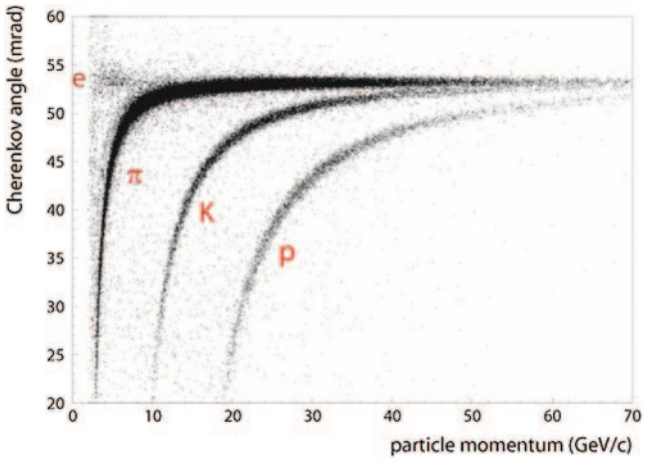

Fig. 1. – The use of Cherenkov radiation in the HERA-B experiment resulted in a very precise determination of the identity of the particles. In the figure the distribution of reconstructed Cherenkov angles is plotted as a function of particle momentum [1].

momentum, the identity of the particle is determined. Although the number of detected photons is low (of the order of about ten photons), the performance of such an identification method is excellent (fig. 1).

2. – Detection of annihilation gammas in a Cherenkov radiator

The Cherenkov effect can also be used in Positron Emission Tomography (PET), one of the most important medical imaging modalities. In PET, a distribution of $\beta+$ labeled biomarker is reconstructed from two nearly co-linear gamma-rays produced during $\beta+$ annihilation, which are detected by position-sensitive gamma detectors. In standard PET, only the detection position of both γ-rays is measured, and the annihilation point probability is constant along the whole line of response (LOR), which leads to a higher background in the image. In the Time-Of-Flight PET, also the arrival time of the detected gamma-rays is measured, resulting in improved contrast of the images, if the time resolution is sufficient. The time resolution Δt is directly related to the position resolution Δx along the line of response,

$$\Delta t \approx 66 \text{ ps} \rightarrow \Delta x = \frac{c\Delta t}{2} \approx 1 \text{ cm}. \tag{3}$$

The most advanced commercial PET imagers are reaching coincidence resolving time of about 200 ps [2]. Only with small isolated scintillation crystals of the size of about 3 mm × 3 mm × 3 mm a coincidence resolving time below 100 ps was measured [3], but the demonstrated performance has not been demonstrated yet in larger systems.

The standard PET detectors employ scintillators where the annihilation gamma-ray is first converted via photo effect to a fast electron. During stopping, the optical photons are emitted and detected by a photodetector at the crystal exit, which converts the photons into electrical pulses. The uncertainty in the arrival time measurements limits the time resolution of such a camera. The main uncertainty contributions are scintillation

TABLE I. – *Properties of several scintillation materials used for the detection of annihilation gamma-rays.*

	BGO	LSO	$LaBr_3$(Ce)
Density ρ (g/cm^3)	7.1	7.4	5.1
Atn. coeff. $\mu_{511\,\mathrm{keV}}$ (cm^{-1})	0.96	0.87	0.43
Photofraction for 511 keV	0.41	0.32	
Decay time (ns)	300	40	17
Light yield (N/511 keV)	3000	15000	30000

emission time spread, characterized by rise and decay time constants, optical photon travel time spread in the crystal, the intrinsic time resolution of the photosensor, and time resolution of the readout electronics used to digitize electrical signals. In table I, properties impacting the gamma detection of several scintillators are shown. Note the long scintillation decay time of the order of 10 ns compared to the coincidence resolving time of 66 ps to localize the source to 1 cm.

Limitation due to delayed scintillation light can be avoided by using Cherenkov light, which is prompt since the electron from the photo effect emits photons in less than 1 ps. The disadvantage of such an approach is a small number of Cherenkov photons N that are produced per interaction. For example, for a 1 cm thick radiator only about 8 photons are emitted in the energy interval of about $\Delta E = 1\,\mathrm{cm}$,

$$N = \frac{370}{\mathrm{eV\ cm}} \Delta E \sin^2\theta_{Ch} \approx 370 \times 0.01 \times 2 \times 0.75 = 8. \tag{4}$$

To detect them, we need a photosensor capable of single-photon detection. Unfortunately, there are only several single-photon photosensors with an intrinsic timing resolution that meets the TOF-PET requirements. The examples are microchannel plate photomultipliers and silicon photomultipliers.

A 511 keV gamma-ray is converted to an electron in a high Z material. In a search for a suitable Cherenkov radiator, which is not scintillating, we selected lead fluoride PbF_2. It is an excellent candidate for the detection of annihilation gammas due to its high gamma stopping power. A high fraction of gamma-rays interacts with the matter through photo effect. Besides, electrons with maximal kinetic energy produce more Cherenkov photons. In addition, the lead fluoride has a high optical transmission for visible and near UV Cherenkov photons. Lead fluoride properties, compared to LYSO and $LaBr_3$ scintillators are shown in table II.

TABLE II. – *Properties of* PbF_2 *compared to* LYSO *and* $LaBr_3$.

	ρ (g/cm^3)	Refractive index n	Cherenkov threshold (keV)	Cut-off λ (nm)	Atten. length (cm)	Photo-fraction
PbF_2	7.77	1.82	101	250	0.91	46%
LYSO	7.4				1.14	32%
$LaBr_3$	5.1				2.23	15%

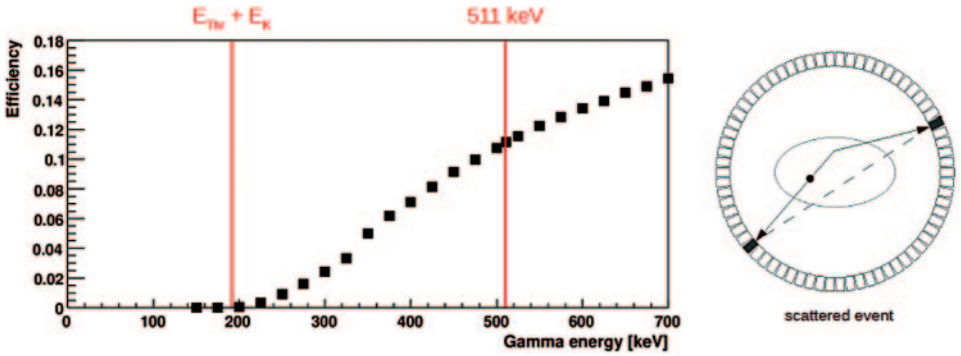

Fig. 2. – Efficiency for gamma-ray detection as a function of gamma energy. Note the intrinsic suppression of low energy gamma events, which are due to Compton scattering in the tissue [4].

In scintillation-based gamma detectors a lot of scintillation photons are detected, their number is proportional to the gamma energy. By accepting only photo-peak events, the gamma-rays scattered in tissue are rejected. This is not the case in Cherenkov-based gamma detectors, where only a few Cherenkov photons are detected, and we have no energy information on the interacting gamma-ray. However, due to the threshold property of Cherenkov radiation and the dependence of a number of emitted photons on the energy, we get an intrinsic suppression of scattered events, since the efficiency drops with gamma energy (fig. 2).

3. – Microchannel plate photomultipliers

Intrinsic timing resolution of photomultipliers, widely used for the detection of photons, is not sufficient for a radiation source localization at the level of cm. Microchannel plate photomultipliers (MCP-PMTs), on the other hand, have excellent timing properties, reaching a single photon timing resolution of 50 ps. We used them in our pioneering experiment, where we positioned two Cherenkov radiation-based gamma detectors in a back-to-back configuration [4]. We used PbF_2 crystals of the size of 25 mm × 25 mm × 5 (15) mm coupled to two MCP-PMTs with a photosensitive area of $22.5 \times 22.5\,mm^2$. For the timing measurements, we painted the crystals with black paint to reduce reflected photons which have delayed arrival to the photosensor. With such an arrangement, we were able to measure a timing resolution of 70 ps FWHM for 5 mm long crystals and 100 ps for 15 mm long crystals. For the efficiency determination, we wrapped the PbF_2 radiator in Teflon and measured an efficiency of about 6% for the annihilation gamma to be detected in a single detector. This number should be compared to an efficiency of about 30% for the conventional LSO-based gamma detectors. We attribute part of the low detection efficiency to the low photo-cathode quantum efficiency of the used MCP-PMTs.

With a 4×4 array of black painted PbF_2 crystals coupled to the multichannel MCP-PMT, we were able to image two ^{22}Na point sources, positioned 2 cm apart. A simple, very fast most-likely-point (MLP) method already gave a reasonable image of the source (fig. 3).

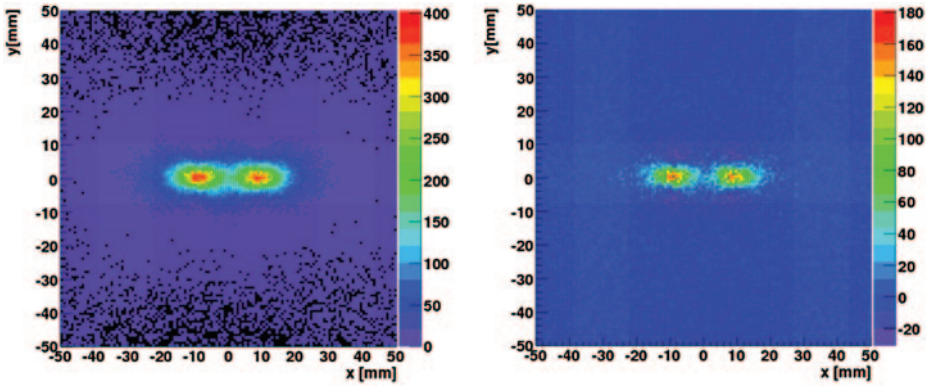

Fig. 3. – Images of two ^{22}Na point sources at positions ± 10 mm, reconstructed with the most-likely-point method (left) and with an additional filtering (right).

4. – Cherenkov-light–based PET scanner

Lead fluoride PbF_2 is not a scintillator and is considerably cheaper than PET scintillators, *e.g.*, LYSO. By using it for gamma detection in PET, one could build a cheaper standard size PET scanner. Another, even more significant, potential is its use in total/half body scanners that have just recently been put in operation [5]. By extending the axial field of view from 20 cm to 200 cm, we can achieve a 6-fold increase in signal to noise ratio as shown by recent results [6]. With such a device, we could either achieve a better image quality or shorten the scanning time or inject less activity. For example, by reducing the injected activity from 8 mSv to 0.2 mSv, one could use the imaging technique also in neonatal diagnostics. The spread of such devices is limited due to extremely high device costs. Decreasing them would have a very high impact on the use of such devices. In addition, the use of lead fluoride would also result in a smaller parallax error due to smaller attenuation length.

On the other hand, although MCP-PMTs have excellent timing, their production is costly. Also, even when using MCP-PMTs with better quantum efficiency, the gamma detection efficiency is smaller compared to the silicon photomultipliers, photosensors that are penetrating the market now and are also much easier to operate.

One possibility is the use of Cherenkov-light–based modules composed of the lead fluoride PbF_2 crystal arrays and silicon photomultipliers. In our work we wanted to address the questions of whether a PET scanner build from such modules would be feasible and whether silicon photomultipliers can be used for efficient light detection of single photons.

Silicon photomultipliers have much higher photon detection efficiency (PDE) compared to other photosensors, they are easier to operate and are much cheaper compared to vacuum devices. They are also insensitive to the magnetic field, which enables their potential use in multimodality devices combined with magnetic resonance imaging. They have, however, also drawbacks. First, their single-photon timing resolution is worse than the MCP-MPT one. The timing resolution of 3 mm $\times$ 3 mm devices is currently limited to around 200 ps FWHM. Second, the silicon photomultipliers have very high dark count rates, which are around 100 kHz/mm^2. These can be mitigated by operating the devices at a lower temperature since the rate decreases exponentially with the temperature.

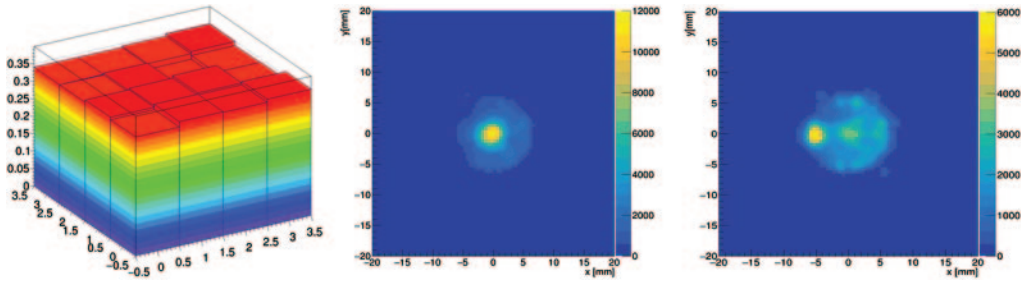

Fig. 4. – Efficiency for the detection of gamma-ray for a single 4×4 array (left). Image reconstruction without time-of-flight information: a ^{22}Na point source in the center (middle), the source displaced by 10 mm (right).

Nevertheless, we decided to test the silicon photomultipliers as light sensors for the detection of Cherenkov photons in the Cherenkov PET device. We first determined a single side efficiency of about 30% with single Teflon wrapped lead fluoride PbF_2 crystals of size $5 \times 5\,\mathrm{mm}^2$ coupled to Sensl SiPM $3 \times 3\,\mathrm{mm}^2$ [7]. Then we determined the timing resolution in the same setup with black painted crystals. The best timing that we obtained was 300 ps with AdvanSiD NUV SiPMs [8]. Note that the experimental system was cooled down to $-25\,^\circ$C to reduce dark counts and correspondingly the number of random coincidences.

Based on the promising results, we built two 4×4 arrays of PbF_2 crystals of size $3 \times 3 \times 15\,\mathrm{mm}^3$ and coupled them to two Hamamatsu arrays S13361-3075 of photosensors. We tested the modules in a setup with a rotating source in the middle to form a virtual PET ring with a diameter of about 10 cm. We connected the output signals to an EASIROC multi-channel electronic module [9]. With such a setup, we measured the 35% average efficiency for a single module, close to what we measured in the single crystal setup (fig. 4). The time resolution of the electronics used for the test was not sufficient for the timing measurements at the precision we want to achieve, so the coincidence timing resolution was not measured in this setup. We are following the design of the multi-channel electronic chips that would enable precise timing measurements of single-photon signals.

To explore the possibilities for the use of Cherenkov PET devices, we have further investigated how we can combine both options by studying other contributions to the timing measurements.

5. – Limitations of fast timing

Although Cherenkov photons are produced promptly, they still need time to reach the photosensor. Their time of flight is higher than the time of flight of gamma-rays due to different velocity of light for visible photons (fig. 5). Because of the non-negligible thickness of the radiator, the difference in time of flight can be significant and impacts the intrinsic travel time spread due to different gamma interaction depths. For example, for a radiator with a refractive index n of 1.8 and thickness d of 15 mm, the time of flight of optical photons produced at the entrance of the crystal, which then propagate to the photosensor downstream of the crystal is

$$t = \frac{dn}{c_0} = 90 \text{ ps}, \tag{5}$$

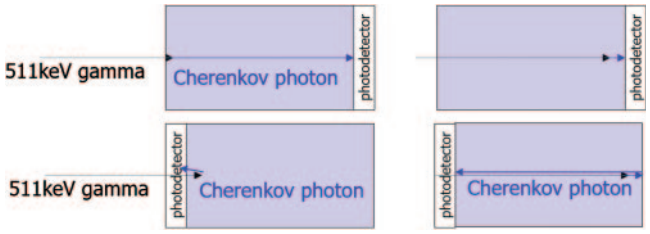

Fig. 5. – The time of arrival of Cherenkov photon depends on their production position and on the position of the photosensor: Cherenkov photons are produced at the entrance (left) and at the exit (right). The photosensor is positioned downstream (above) or upstream (below) of the gamma-ray direction.

whereas for photons that are produced close to the sensor, the effective time equals the delayed gamma interaction time,

$$t = \frac{d}{c_0} = 50 \text{ ps}. \tag{6}$$

The time difference Δt is in this case 40 ps.

In the case when the photosensor is located on the upstream side of the crystal, the difference enlarges. The photon produced at the crystal entrance is immediately detected, while the time of arrival of the photon, produced with a delay at the downstream side is

$$t = \frac{d}{c_0} + \frac{dn}{c_0} = 140 \text{ ps}. \tag{7}$$

Evidently, such a geometry is worse than the downstream one. Note that this limitation is common to all high-speed light emission mechanisms, *i.e.*, also to the scintillation light.

One possibility to reduce the effect of timing spread is by using a multi-layer configuration with shorter crystals (fig. 6).

We performed simulations of such a multi-layer configuration arranged in a whole-body PET scanner with 20 cm axial coverage and compared it to the Siemens Biograph state of the art scanner based on LSO crystals and reaching 214 ps coincidence timing resolution [2, 10]. We used GATE [11] to simulate the system and CASToR for iterative time-of-flight reconstruction [12].

We arranged an array of three layers of $5 \times 5 \times 5\,\text{mm}^3$ of PbF_2 black painted crystals coupled to $5 \times 5\,\text{mm}^2$ big silicon photomultipliers and simulated photosensors with a 0 ps

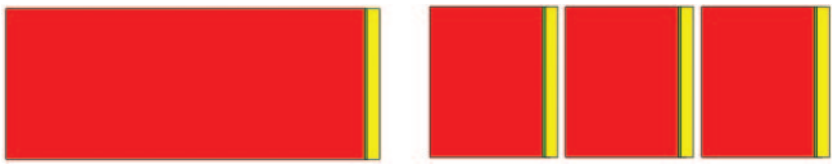

Fig. 6. – The timing error due to the timing spread in the crystal can be reduced by segmenting the gamma-ray detector.

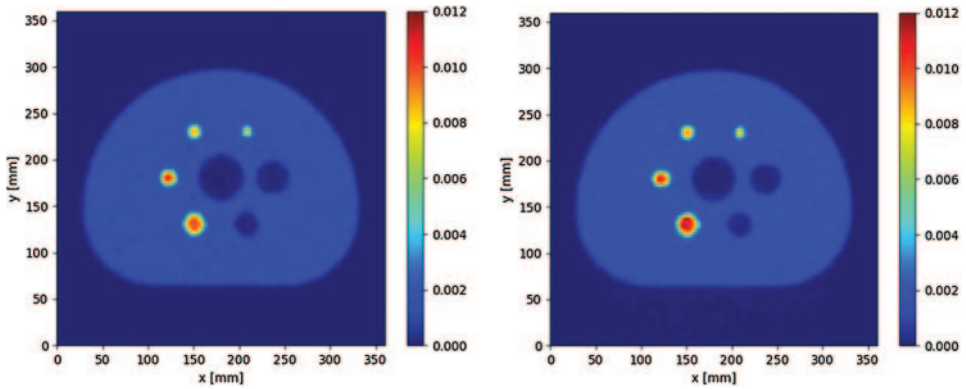

Fig. 7. – Reconstructed images with MLP reconstruction and correction of background attenuation: LSO with CTR 200 ps (left), PbF_2 photosensor TTS 100 ps (right), acquisition time 7.5 s, injected activity of 300 MBq.

time spread and got a coincidence time resolution (CTR) of 22 ps FWHM. Such a resolution would boost the detector performance of the PET system compared to the current ones. With a realistic photodetector timing of 100 ps included in the simulation [3], we obtained a coincidence time resolution of 143 ps FWHM. The images obtained with a whole-body PbF_2 Cherenkov TOF-PET scanners are competitive with the image obtained with a whole-body LSO TOF-PET scanner (fig. 7).

6. – Other ideas

The other possibility to reduce the effect of timing spread in the crystal is to measure the depth of gamma interaction (DOI). By measuring it, we would additionally improve the parallax error. This concept has been proposed by the CALIPSO project [13]. They are using a high Z liquid, Tri-Methyl Bismuth (TMBi), for gamma conversion and dual-mode readout with timing for the detection of Cherenkov light. They measure the ionization to determine the gamma-ray energy and to determine the interaction point (2D pixels for charge collection and drift time). The detector is an excellent example of technology transfer from high energy physics to medical imaging.

Another idea proposed in the Cherencube project [14] is the extension of the readout to all six sides of the crystal.

The combination of Cherenkov and scintillation light where the Cherenkov photons are used for fast timing and the scintillation photons for energy measurements was discussed by [15]. They proposed the use of the bismuth germanium oxide (BGO). By measuring the Cherenkov photons one would achieve a good timing measurement, while still maintaining high efficiency for gamma-ray conversion. The scintillator has a low price, high density, and a large ratio of photo effect undergoing gammas.

7. – Conclusions

Lead fluoride Cherenkov radiation-based annihilation gamma detectors offer a promising method for TOF-PET measurements. They can be used to build potentially cheaper standard scanners. However, their use might have an even more significant impact on

total body scanners, where their use also has another benefit: a reduction of the parallax error, because of the use of shorter crystals due to a shorter attenuation length of lead fluoride PbF_2.

Silicon photomultipliers have been proven to work as sensors for Cherenkov light originating from annihilation gamma absorption. The single side efficiency is comparable to LSO scintillator-based detectors; however, their intrinsic time resolution is not yet sufficient. Further improvements in the timing of silicon photomultipliers and front-end electronics would further boost this interesting detection method.

* * *

The author acknowledges the support from the Slovenian Research Agency research grant Nos. J1-9124, J1-5436, J1-9340, and research core funding No. P1-0135.

REFERENCES

[1] Ariño I. *et al.*, *Nucl. Instrum. Methods A*, **516** (2004) 445.
[2] Siemens Biograph Vision Technical Sheet, retrieved April 2019, `http://www.siemens-healthineers.com`.
[3] Gundacker S. *et al.*, *Phys. Med. Biol.*, **64** (2019) 055012.
[4] Korpar S., Dolenec R., Križan P., Pestotnik R. and Stanovnik A., *Nucl. Instrum. Methods A*, **732** (2013) 595.
[5] Cherry Simon R., Jones Terry, Karp Joel S., Qi Jinyi, Moses William W. and Badawi Ramsey D., *J. Nucl. Med.*, **59** (2018) 3.
[6] Badawi Ramsey D., Shi Hongcheng, Hu Pengcheng, Chen Shuguang, Xu Tianyi, Price Patricia M., Ding Yu, Spencer Benjamin A., Nardo Lorenzo, Liu Weiping, Bao Jun, Jones Terry, Li Hongdi and Cherry Simon R., *J. Nucl. Med.*, **60** (2019) 299.
[7] Korpar S., Dolenec R., Križan P., Pestotnik R. and Stanovnik A., *Nucl. Instrum. Methods A*, **654** (2011) 532.
[8] Dolenec R., Korpar S., Križan P., Pestotnik R. and Verdel N., *IEEE Trans. Nucl. Sci.*, **63** (2016) 2478.
[9] Nakamura I., Ishijima N., Hanagaki K., Yoshimura K., Nakai Y. and Ueno K., *Nucl. Instrum. Methods A*, **787** (2015) 376.
[10] Consuegra D., Korpar S., Križan P., Pestotnik R., Razdevšek G. and Dolenec R., *Phys. Med. Biol.*, **65** (2020) 055013.
[11] Strul D., Santin G., Lazaro D., Bretonad V. and Morel C., *Nucl. Phys. B. (Proc. Suppl.)*, **125** (2003) 75, see also `http://www.opengatecollaboration.org`.
[12] Merlin Thibaut, Stute Simon, Benoit Didier, Bert Julien, Carlier Thomas, Comtat Claude, Filipovic Marina, Lamare Frédéric and Visvikis Dimitris, *Phys. Med. Biol.*, **63** (2018) 5505.
[13] Yvon D. *et al.*, *IEEE Trans. Nucl. Sci.*, **61** (2014) 60.
[14] Somlai-Schweiger I. and Ziegler S., *Med. Phys.*, **42** (2015) 1825.
[15] Brunner S. E. and Schaart D. R., *Phys. Med. Biol.*, **62** (2017) 4421.